

Rapid Temporal Variability of Faculae: High Resolution Observations and Modeling

B. De Pontieu

*Lockheed Martin Solar and Astrophysics Lab, 3251 Hanover St., Org. ADBS, Bldg. 252,
Palo Alto, CA 94304, USA*

`bdp@lmsal.com`

M. Carlsson¹

*Institute of Theoretical Astrophysics, University of Oslo, PO Box 1029 Blindern, 0315
Oslo, Norway*

`mats.carlsson@astro.uio.no`

R. Stein

*Department of Physics and Astronomy, Michigan State University, East Lansing, MI
48824, USA*

`stein@pa.msu.edu`

L. Rouppe van der Voort¹

*Institute of Theoretical Astrophysics, University of Oslo, PO Box 1029 Blindern, 0315
Oslo, Norway*

`rouppe@astro.uio.no`

M. Löfdahl

*Institute for Solar Physics of the Royal Swedish Academy of Sciences, AlbaNova University
Center, 106 91 Stockholm, Sweden*

`mats@astro.su.se`

¹Also at: Center of Mathematics for Applications, University of Oslo, P.O. Box 1053, Blindern, N-0316 Oslo, Norway

M. van Noort²

*Institute of Theoretical Astrophysics, University of Oslo, PO Box 1029 Blindern, 0315
Oslo, Norway*

`noort@astro.su.se`

Å. Nordlund

Niels Bohr Institute, Juliane Maries Vej 30, 2100 Copenhagen, Denmark

`aake@astro.ku.dk`

G. Scharmer

*Institute for Solar Physics of the Royal Swedish Academy of Sciences, AlbaNova University
Center, 106 91 Stockholm, Sweden*

`scharmer@astro.su.se`

ABSTRACT

We present high resolution G-band observations (obtained with the Swedish 1 m Solar Telescope) of the rapid temporal variability of faculae, which occurs on granular timescales. By combining these observations with magneto-convection simulations of a plage region, we show that much of this variability is not intrinsic to the magnetic field concentrations that are associated with faculae, but rather a phenomenon associated with the normal evolution and splitting of granules. We also show examples of facular variability caused by changes in the magnetic field, with movies of dynamic behavior of the striations that dominate much of the facular appearance at 0.1'' resolution. Examples of these dynamics include merging, splitting, rapid motion, apparent fluting, and possibly swaying.

Subject headings: magnetic fields — Sun: photosphere — Sun: chromosphere

²Now at: Institute for Solar Physics of the Royal Swedish Academy of Sciences, AlbaNova University Center, 106 91 Stockholm, Sweden

1. Introduction

Faculae are ubiquitous, bright, and small features that are observed close to the solar limb. They are associated with magnetic field concentrations that are most often part of active region plage. Because of their close association with the Sun’s variable magnetic field, the excess brightness of faculae plays a dominant role in the increased solar irradiance during periods of high solar magnetic activity (e.g., Fligge et al. 2000; Walton et al. 2003). A detailed understanding of faculae can thus shed light on one of the main drivers of solar irradiance variability.

Our understanding of faculae and what is behind their excess brightness has been greatly increased in the past few years. Recent observations with extremely high spatial resolution ($\sim 0.1''$) from the Swedish 1 m Solar Telescope (SST) on La Palma, Spain, have revealed faculae to be highly structured features with a three dimensional appearance, that show a clear asymmetry along the limbward direction (Lites et al. 2004). A sharp, dark lane usually appears on the disk center side of the faculae, which themselves are spatially extended in the limbward direction by $0.5\text{--}1''$, and usually show some striations in the direction perpendicular to the limbward direction. The combination of these unprecedented observations with interpretation using synthetic images derived from advanced 3D radiative magnetoconvection simulations have allowed significant advances in our understanding of how faculae are formed (Keller et al. 2004; Carlsson et al. 2004; Steiner 2005; Okunev & Kneer 2005).

From these theoretical calculations it has become clear that the increased brightness associated with faculae is caused predominantly by the lower density within the evacuated magnetic field concentrations that are associated with faculae. The lower density in regions of strong magnetic field arises from the horizontal pressure equilibrium of flux concentrations with the less magnetized surroundings. Because of the lower density and associated lower opacity, an observer can see deeper layers that are part of the granular wall in the limbward direction of the magnetic flux concentration (Keller et al. 2004). These deeper layers of the granule are at a higher temperature, which can explain the excess brightness (Spruit 1976, 1977; Carlsson et al. 2004). The limbward spatial extent of the faculae depends in part on the height of the granule on the disk center side of the flux concentration. Depending on the exact viewing angle and granular geometry, the denser granule can “block” some of the light rays that would otherwise have reached the observer, leading to a different facular visibility. The origin of facular brightening is nicely illustrated in Fig. 4 of Keller et al. (2004). This figure also shows how the dark lane on the disk center side of the faculae is formed in the relatively cool regions inside the flux concentration and above the granule at the disk center side of the concentration.

While faculae are typically elongated in the limbward direction, more generally they

are extended in the local vertical direction. Striations typically appear in the direction perpendicular to the limbward direction, or more generally in the local horizontal direction, with patterns of bright, elongated features alternating with relatively darker features on spatial scales of order $0.2''$. As shown in §4.3, these striations can be explained in terms of spatial variations in the magnetic field strength, and associated variations in evacuation, density and thus opacity, which leads to brightness variations as described in the above. To our knowledge, none of the existing numerical simulations have obtained high enough spatial resolution to fully explain why the magnetic field itself is structured at such small spatial scales.

All of the above work has been static, as it is based on snapshots of faculae (e.g., Lites et al. 2004), with none of the observational work so far describing the dynamics of faculae. Recently Okunev & Kneer (2005) described some dynamics of polar faculae at a resolution of $0.25''$. Here we describe the first observations that show the dynamics of faculae at very high spatial resolution ($\sim 0.1''$). Our G-band observations (described in §2) show that the dynamics of faculae are amazingly complex and highly variable on granular timescales of order minutes. The intricacies of these facular dynamics, never before imaged at this spatial resolution, are the subject of this work. We combine observations and 3D radiative magneto-convective simulations (described in §3) to show that much of this facular variability is not intrinsic to faculae or a function of the magnetic field, but rather a phenomenon associated with the normal evolution and splitting of granules. This is because faculae are a window into a hot, granular wall in the background. As a result, the facular brightness directly depends on the temperature of the background granular wall, which changes because of the granular evolution on time scales of minutes.

We describe the general properties of the facular dynamics in §4.1, and in §4.2 we focus on the appearance and disappearance of dark bands that appear to "wipe out" faculae on very short time scales. The influence of granular temperature stratification and its dynamical evolution on the facular brightness implies that it is very difficult to study flux concentration dynamics using G-band time series. In §4.3, we nevertheless describe some examples of flux concentration dynamics which include merging, splitting, rapid motion, apparent fluting, and perhaps even swaying.

2. Observations

The observational data were taken on 16 June 2003 from 08:44 to 09:47 UT using adaptive optics at the Swedish 1 m Solar Telescope. The G-band 4302 \AA time series was corrected for dark current and flat field. We used multi-frame blind deconvolution of three

images taken within 20 seconds (Löfdahl 2002; van Noort, Rouppe van der Voort & Löfdahl 2005), to obtain images with higher and more consistent image quality throughout the field of view. After this image processing, we rigidly co-aligned the time series using cross correlation. Destretching was performed to remove the geometrical distortions component of anisoplanatic seeing of the Earth’s atmosphere. Finally, subsonic filtering using Fourier transforms (with 4 km/s as cutoff) was used to remove the effects of p-mode oscillations.

The final time series contains 158 images with a time cadence of about 24 seconds. Each image is 1920x1920 pixels with an image scale of 0.041" per pixel. The resolution of many of the images is close to the diffraction limit ($\sim 0.1''$) and most images have a spatial resolution better than 0.2".

The field of view of the time series of the G-band images contains a small sunspot with a large region of adjacent plage (see Fig. 1), both part of NOAA active region 10380. This active region was located at an average $\mu = \cos \theta = 0.65$, with θ the angle between the line-of-sight and the local vertical. All images have been rotated to have the direction of the limb upwards.

3. Simulations

The three-dimensional magnetoconvection simulations include LTE ionization and excitation in the equation of state and nongray LTE radiation transfer in the energy balance. These simulations were described in some detail in Carlsson et al. (2004). They cover a small region of 6 x 6 Mm, sufficient to include one mesogranule and many granules, and extend from the temperature minimum down to a depth of 2.5 Mm below $\tau_{500} = 1$. The grid resolution is 25 km horizontally and varies from 15 km in the upper layers to 35 km vertically in the lower layers (Stein & Nordlund 1998). Generally, only features larger than about 4-5 grid steps may be expected to be adequately resolved. The simulation was started with a uniform vertical magnetic field of 250 G superposed on a snapshot of nonmagnetic convection and then allowed to relax. The total length of the MHD simulation time series is 2610 s. Convective motions exist on all scales from granules to giant cells with larger scales dominant at larger depths. The largest scales that exist in our computational domain are the mesogranule scales. The magnetic field is quickly swept to the boundaries of these deeper lying mesogranules and concentrated to typical strengths of 1.7 kG at the level $\tau_{500} = 1$. In contrast, the intergranule lanes often contain weak mixed polarity field (Fig. 2).

The emergent spectrum was calculated in LTE for a wavelength interval of 3 nm width centered on 430.68 nm (G band). Molecular equilibrium was calculated including all diatomic

molecules of hydrogen, carbon, nitrogen, and oxygen. For the spectrum calculation, 1364 frequency points were used. The calculated emergent intensities were multiplied with a filter transmission curve (from the SST) with a central wavelength as above and FWHM of 1.08 nm, and integrated over wavelength to create synthetic images in the G band.

4. Results

4.1. General

The dynamics of faculae when observed in the G band at a spatial resolution of $0.1''$ are extremely complicated and difficult to interpret without guidance from 3D radiative MHD simulations. Unlike the dynamics of G-band bright points closer to disk center, it is almost impossible to track individual "elements" for longer than just a few minutes. Both the brightness and identity of faculae undergo drastic changes in the course of just a few minutes. This is nicely illustrated in Fig. 3 which shows a tiny patch of plage, the size of only 2 or 3 granules across. This plage subregion was chosen because the facular dynamics are typical for our observations. In this case, faculae that are clearly identifiable at $t = 0$ s, e.g., at $(0.5'', 1.5'')$ or $(1.5'', 2'')$ can no longer be identified after $t = 440$ s. Visual inspection of Fig. 3 and movies of other regions show that these rapid changes in facular visibility are intimately tied to the dynamics of the granules surrounding the faculae. In the case of Fig. 3, a granule forms at the top of the field of view which influences the faculae at $(1.5'', 2'')$ a few minutes later.

Our observations show that faculae generally lack a consistent "identity", sometimes even changing into pointlike brightenings, followed by a return of larger facular brightenings. For example, faculae are clearly visible in Fig. 4 at $(1.5'', 1.5'')$ at $t = 0$ s. These wispy features rapidly change and seem to shrink with time, until only a thin line of pointlike brightenings remains at $t = 538$ s. This drastic change in visibility of the faculae coincides with the evolution of a granule just limbward of the faculae.

These pointlike brightenings should not be confused with the G-band bright points (BP's) that are observed around disk center. The visibility mechanism is different. With G-band BP's at disk center, we see deep into the vertical temperature structure of a flux concentration. With faculae we see the temperature structure of a separate physical structure behind the flux concentration. In addition, a G-band BP at disk center is bright because the flux concentration is small enough to get heated from the sides. Larger concentrations have a different appearance at disk center: they look like flowers, ribbons and micro-pores with a bright edge. These larger concentrations look like faculae towards the limb. Most

disk-center BP’s do not have enough flux in their vicinity to evolve into a ribbon (at disk center), or to appear as faculae close to the limb. When faculae evolve to thin strings of pointlike brightenings (e.g., Fig. 4), this is because of the evolution behind and in front of the flux concentration. The object would still look like a ribbon at disk center, and not like a string of bright points.

While faculae have been interpreted as a proxy for magnetic field concentrations, it is clear from these high resolution observations that at very small spatial scales of order less than $0.5''$ and on timescales of order minutes, identifying changes in facular visibility with dynamics of magnetic field concentrations can be problematic.

What is behind these complicated dynamical changes in facular visibility? They are a natural consequence of how G-band images are formed as described in §1 (Keller et al. 2004; Carlsson et al. 2004; Steiner 2005). Timeseries of synthetic G-band images based on numerical simulations of magneto-convection in plage-like conditions (see §3) show facular dynamics that are very similar to those observed with the SST. This is illustrated in Fig. 5 where the faculae at $(1.5'', 1.5'')$ rapidly shrink and disappear within 240 seconds. Other faculae in these simulations also undergo rapid and drastic changes. Detailed analysis of the numerical simulations indicate that the facular dynamics are dominated by granular dynamics, rather than by the dynamics of magnetic field concentrations. The relative excess of brightness in G-band faculae is caused by the fact that the evacuated magnetic flux concentrations provide windows into deeper layers. When a magnetic flux concentration is viewed closer to the limb, an observer sees more and more deeply into the hotter layers of the granule at the limbward side of the flux concentration. As the granule evolves, its temperature stratification changes significantly. The change in background temperature structure of the granule will cause a corresponding variation of the G-band brightness of the faculae associated with the evacuated flux concentration. Since granules turn over on timescales of five to ten minutes, it is clear that facular dynamics will occur on this timescale as well. The numerical simulations clearly show that the magnetic field is dynamic, since the flux concentrations are continuously buffeted by convection. However, the simulations also indicate that most of the facular dynamics are caused by changes in visibility directly associated with variations in viewing angle and “background” granular flows and temperature stratification.

4.2. Dark Bands

A ubiquitous feature of G-band movies of faculae are “dark bands”, which are generally parallel to the solar limb. These features typically appear limbward of faculae and seem

to "erase" the faculae as they approach them. In other words, the dark bands sweep over the bright faculae which, as a result, gradually decrease in spatial extent in the limbward direction and in overall brightness. Several minutes after passage of the dark bands, the faculae typically regain their brightness. In other words, the dark bands do not seem to fundamentally change the underlying magnetic field configuration. Figures 6 and 7 are examples of dark bands. In Fig. 6 a dark band appears at $(1.2'', 2'')$ at $t = 0$ s. By $t = 342$ s, it has encroached significantly on the faculae just "below" (or towards disk center) which have shrunk and becomes less bright as a result. By $t = 538$ s, the faculae have disappeared from view. Another example is shown in Fig. 7 which shows a dark band appearing at $(1.2'', 1.5'')$ at $t = 0$ s. This band erases the faculae at $(1.2'', 1.2'')$ from view by $t = 171$ s. Such behavior is quite ubiquitous in the full dataset of 63 minutes with a majority of faculae undergoing some form of "erasing" by dark bands (usually followed by recovery to brightness) at some point in their lifetime. These dark bands travel at apparent velocities of order 1-2 km/s, as evidenced by the xt-cuts in Fig. 8. The two dark bands illustrated travel at a speed of 1.2 km/s and 1.8 km/s for the left and right hand case respectively. Velocities of order 1.5 km/s are quite normal for convective flows. Indeed, a detailed analysis of the numerical simulations shows that these dark bands are a normal part of the evolution of a granule. Figure 9 shows an example of a dark band extinguishing faculae in the synthetic G-band movies calculated from the 3D MHD magneto-convective simulations. At $t = 0$ the dark band is just above the center of the figure. It moves towards disk center (downwards in the figure) and the faculae are reduced to a weak band at $t = 90$ s. There is also a magnetic flux concentration being advected by the granular flow starting at $(2.3'', 1.5'')$ at $t = 0$, moving to the left and increasing in brightness to reach position $(1.5'', 1.2'')$ at the end of the timeseries.

Dark bands form naturally during the course of the evolution of a granule. The phenomenon is similar to that of an "exploding" granule, except that in this case the breaking up of the granule occurs not in a roughly spherical fashion, but rather more linear. The upward mass flux in the interior of a granule produces an overpressure which drives the horizontally diverging granular flow (Fig. 10). This overpressure also decelerates the interior upflow, which reduces the convective flux. The surface heating decreases below the rate of radiative surface cooling and the surface temperature and brightness decrease (Nordlund 1995). Where the granular flow becomes nearly horizontal the upward convective flux is also reduced, which leads to the formation of dark lanes. The horizontal flow is unstable and becomes undulating (fig 11). In the downward phase of the undulations the energy flow to the surface is reversed, which enhances the surface cooling and strengthens the dark lanes. Figure 12 shows a space-time cut through a dark band. The contours show the total enthalpy plus kinetic energy flux. The decrease in the flux leads to the formation of a dark

lane which becomes darker when the flux reverses (becomes downward) and removes energy from, rather than providing energy to, the surface. The dark band is swept along by the horizontally diverging granular flow into the magnetic concentration, where it temporarily dims the faculae. When this elongated region of reduced temperature reaches the magnetic field filled intergranular lane, the line-of-sight reaches into the cooler layers which appears to wipe out the usual excess in brightness observed in faculae. Faculae are the bright walls of the center facing sides of granules, so only dark lanes advected away from the limb toward the Sun center will lead to facular dimming.

4.3. Variability caused by magnetic field

In this section we describe examples of facular variability that do not seem to be caused by granular evolution. A full determination of whether all of the G-band dynamics described below are caused by changes in the magnetic field is not possible without magnetogram data (which was not available for this data). However, all of these examples occur in very dense plage regions where granulation is abnormal and convective flows are heavily suppressed. Given the above, it seems that such regions might provide us with the only way of isolating and determining the dynamics of magnetic flux concentrations using G-band images towards the limb. Since it is easier to obtain high resolution G-band data than high-resolution magnetograms at the limb, it is worthwhile to study these examples of apparent flux concentration dynamics.

Figure 13 shows how striated two sets of faculae are (one in the middle, the other in the upper left corner), and how dynamic the number and location of the striations are. Some of the changes are probably caused by atmospheric seeing effects, but it is clear that the faculae in the middle ($x=1.1-1.8''$, $y=1.3''$) go from having three bright striations at $t = 0$ s, to having four around $t = 440$ s. The relatively dark gaps between the bright striations correspond to regions of smaller magnetic flux or weaker magnetic field. This is illustrated in Fig. 14, which shows the synthetic G-band intensity at $\mu = 0.6$, the distance along each ray to optical depth unity and the integrated magnetic field strength down to optical depth unity (all from the 3D MHD simulations). As can be seen from Fig. 14, the relatively dark gaps between the three bright striations are well correlated with lower field strengths at those locations. The spatial modulation in facular brightness can thus be interpreted as a modulation in magnetic field strength. More generally, a modulation in magnetic flux could cause a similar effect on the brightness. This fits well with the formation of G-band faculae as described in §1 and §4: weaker field or flux implies less evacuation, denser plasma, and more opacity. Such regions do not provide as deep of a window into lower-lying regions, and are thus less

bright (see middle panel of Fig. 14). These results are based on numerical simulations, and are also observed in recent SST data that includes magnetograms (Berger et al. 2006). We note that since we do not have access to magnetogram data for our observations, we cannot distinguish whether lower field strength or lower magnetic flux is behind the striations we report on here.

Dynamic behavior of striated faculae is also shown in Fig. 15 where faculae seem to split and merge within a timeframe of five minutes or less. Time lapse movies of these subregions show how the facular striations move in a direction perpendicular to their own long axis with speeds of order 0.5 to 1 km/s. These velocities are similar to those obtained by G-band bright points when observed closer to disk center (Berger et al. 1998). Figure 15 shows how the faculae to the right of $x = 0.4''$ start with three bright striations at $t = 0$ s. By $t = 73$ s, the striation around $x = 0.5''$ seems to have split in two, which is more clearly seen at $t = 148$ s. By $t = 171$ s these striations merge again, leaving only three bright striations to the right of $x = 0.4''$. At the end of this timeseries, it appears as if the merged striation is on the verge of once again splitting up. The view that emerges from these observations is compatible with observations of the behavior of G-band ribbons or bright points at disk center. Those are also seen to split, merge and move rapidly along the intergranular lanes (Berger et al. 2004; Rouppe van der Voort et al. 2005).

A final example of apparent magnetic flux concentration dynamics is presented in Fig. 16 which shows a tiny area ($1''$ by $1''$) of plage. Time lapse movies indicate that the central bright striation seems to sway from right to left and back. Using the diagonal black line in Fig. 16, it seems that the direction of the central bright striation is aligned with the guiding line at $t = 0$ s and later at $t = 195$ s, whereas especially around $t = 97$ s, the axis of the central bright striation makes an angle of order 20 degrees or so with the guiding line. One can speculate that this observation shows the swaying of a photospheric flux concentration, not unlike the swaying seen in some numerical simulations, e.g., those of Steiner et al. (1998). Unfortunately the quality of the current observational data is not quite consistently good enough to make a fully convincing case for this interpretation. Higher-quality datasets with consistent spatial resolution of $0.1''$ close to the limb are necessary to resolve this issue.

5. Conclusions

Faculae change very significantly on timescales of order a few minutes: it is hard to track individual facular elements for longer than just a few minutes. Comparisons between observations and numerical simulations show that most of these facular changes are directly related to those of the granule in the limbward direction of the magnetic flux concentrations

associated with the faculae. This follows naturally from the fact that the evacuated flux concentrations associated with faculae provide a low opacity window into deeper and hotter layers of the granules at their limbward side. As a result, the dark bands that are often observed to "sweep over" and darken or extinguish faculae are related to granular evolution. These dark bands are a phenomenon associated with the splitting of granules. They are visible in G-band data taken at disk center, but are more conspicuous towards the limb. Our conclusions are different from those of Okunev & Kneer (2005). These authors attribute their observations of dynamics of polar faculae to changes in the magnetic field of flux concentrations that respond to external pressure from buffeting by convection, with associated opacity changes. Our higher resolution observations and detailed comparison with numerical simulations shows that these effects are most often dominated by granular evolution.

Only in some cases do facular changes seem to show dynamics of magnetic flux concentrations as opposed to granular dynamics. This occurs only in regions of dense plage where the background granular flows are heavily disturbed and suppressed, thus providing a more stable background intensity than usual plage or network regions. Some of the behavior observed in such regions is reminiscent of that of G-band bright points or ribbons close to disk center: splitting, merging and rapid motion along intergranular lanes. The proximity to the limb does provide one type of observation that is very difficult to obtain at disk center: a flux concentration that apparently sways by about 20 degrees from the vertical, presumably under the influence of convective flows. While the quality of the time series is very good, it is unfortunately not consistently good enough to fully support this interpretation.

BDP was supported by NASA grants NAG5-11917, NNG04-GC08G and NAS5-38099 (TRACE), and thanks the ITA/Oslo group for excellent hospitality. This research was supported by the European Community's Human Potential Programme through the European Solar Magnetism Network (ESMN, contract HPRN-CT-2002-00313), by The Research Council of Norway through grant 146467/420 and through grants of computing time from the Programme for Supercomputing, the National Center for Supercomputer Applications, Michigan State University, and the Danish Center for Scientific Computing. The Swedish 1-m Solar Telescope is operated on the island of La Palma by the Institute for Solar Physics of the Royal Swedish Academy of Sciences in the Spanish Observatorio del Roque de los Muchachos of the Instituto de Astrofísica de Canarias. RFS was supported by NASA grants NNG04GB92G and NAG 5-12450, and NSF grant AST 0205500.

REFERENCES

- Berger, T.E., Löfdahl, M.G., Shine, R.S., Title, A.M., 1998, *ApJ*, 495, 973
- Berger, T.E., Rouppe van der Voort, L.H.M., Löfdahl, M.G., Carlsson, M., Fossum, A., Hansteen, V.H., Marthinussen, E., Title, A., Scharmer, G., 2004, *A&A*, 428, 613
- Berger, T.E., et al., 2006, in preparation
- Carlsson, M., Stein, R.F., Nordlund, Å, Scharmer, G.B., 2004, *ApJ*, 610, L137
- Fligge, M., Solanki, S.K., Unruh, Y.C., 2000, *A&A*, 353, 380
- Hirzberger, J., Wiehr, E., 2005, *A&A*, 438, 1059
- Keller, C.U., Schüssler, M., Vögler, A., Zakharov, V., *ApJ*, 607, L59
- Lites, B.W., Scharmer, G.B., Berger, T.E., Title, A.M., 2004, *Sol. Phys.*, 221, 65
- Löfdahl, M.G., 2002, in *Proc. SPIE 4792, Image Reconstruction from Incomplete Data II*, Bones, Fiddy & Millane, eds., pp. 146-155
- Nordlund, Å, 1995, *Sol. Phys.*, 100, 209
- Okunev, O.V., Kneer, F., 2005, *A&A*, 439, 323
- Rouppe van der Voort, L.H.M., Hansteen, V.H., Carlsson, M., Fossum, A., Marthinussen, E., van Noort, M.J., Berger, T.E., 2005, *A&A*, 435, 327
- Spruit, H.C., 1976, *Sol. Phys.*, 50, 269
- Spruit, H.C., 1977, *Sol. Phys.*, 55, 3
- Steiner, O., Grossmann-Doerth, U., Knölker, M., Schüssler, M., 1998, *ApJ*, 495, 468
- Stein, R.F., Nordlund, Å, 1998, *ApJ*, 499, 914
- Steiner, O., 2005, *A&A*, 430, 691
- van Noort, M.J., Rouppe van der Voort, L.H.M., Löfdahl, M., 2005, *Sol. Phys.*, 228, 191
- Walton, S.R., Preminger, D.G., Chapman, G.A., 2003, *ApJ*, 590, 1088

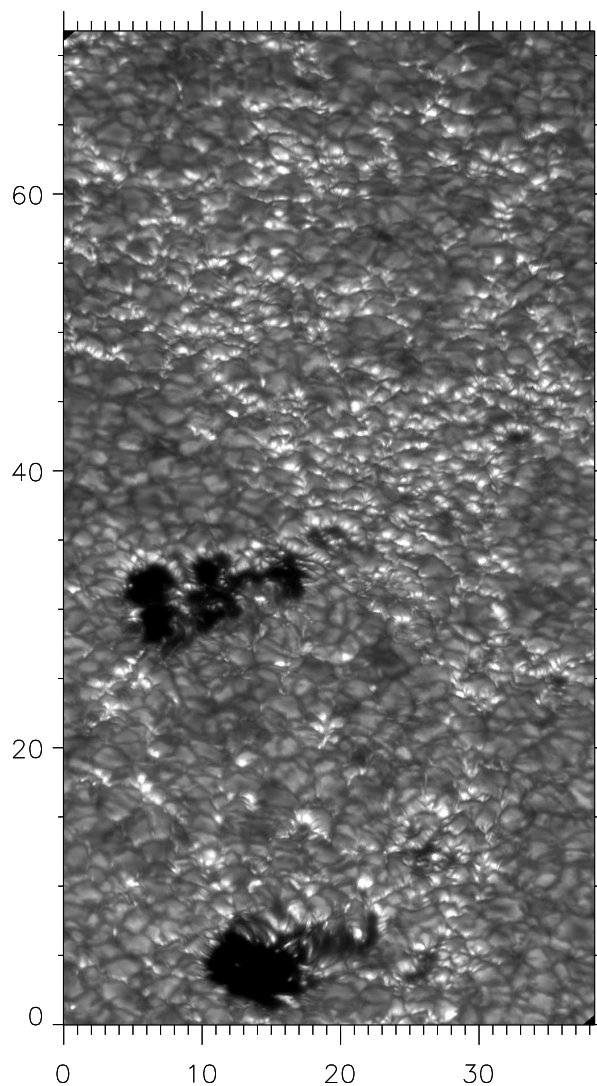


Fig. 1.— Small sunspots and plage in NOAA AR 10380 on 16-June-2003, imaged in the G band 4302 \AA at 09:11:02 UTC at the Swedish 1 m Solar Telescope. Tickmarks are in arcseconds (in all other figures, except where noted differently). The image is rotated so that the limbward direction is up. This is the case for all other figures as well, except where noted. To improve image quality, this image was restored by using multi-frame blind deconvolution on 3 images that were taken very close in time (within 15 s). An mpeg movie is available online.

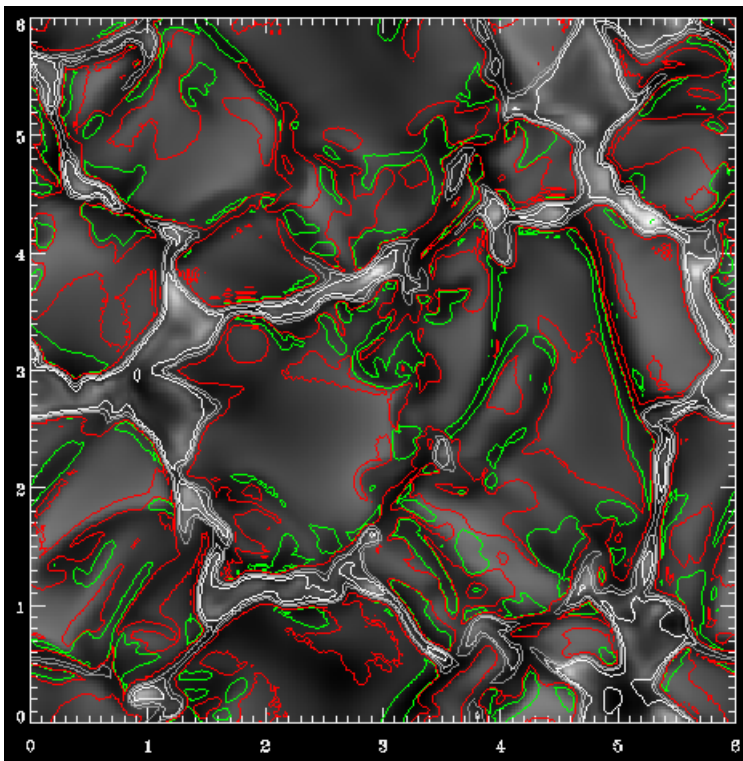


Fig. 2.— Magnetic field strength contours superimposed on G-band intensity image, both from numerical simulations. The contour levels are 0.5, 1.0 and 1.5 kG (dark gray, light gray and white) and ± 20 G (red and green). Kilogauss strength fields are confined to the intergranular lanes at the borders of the underlying meso-granule cell. However, weak fields of both polarities fill most of the intergranular lanes. Tickmarks are in Mm.

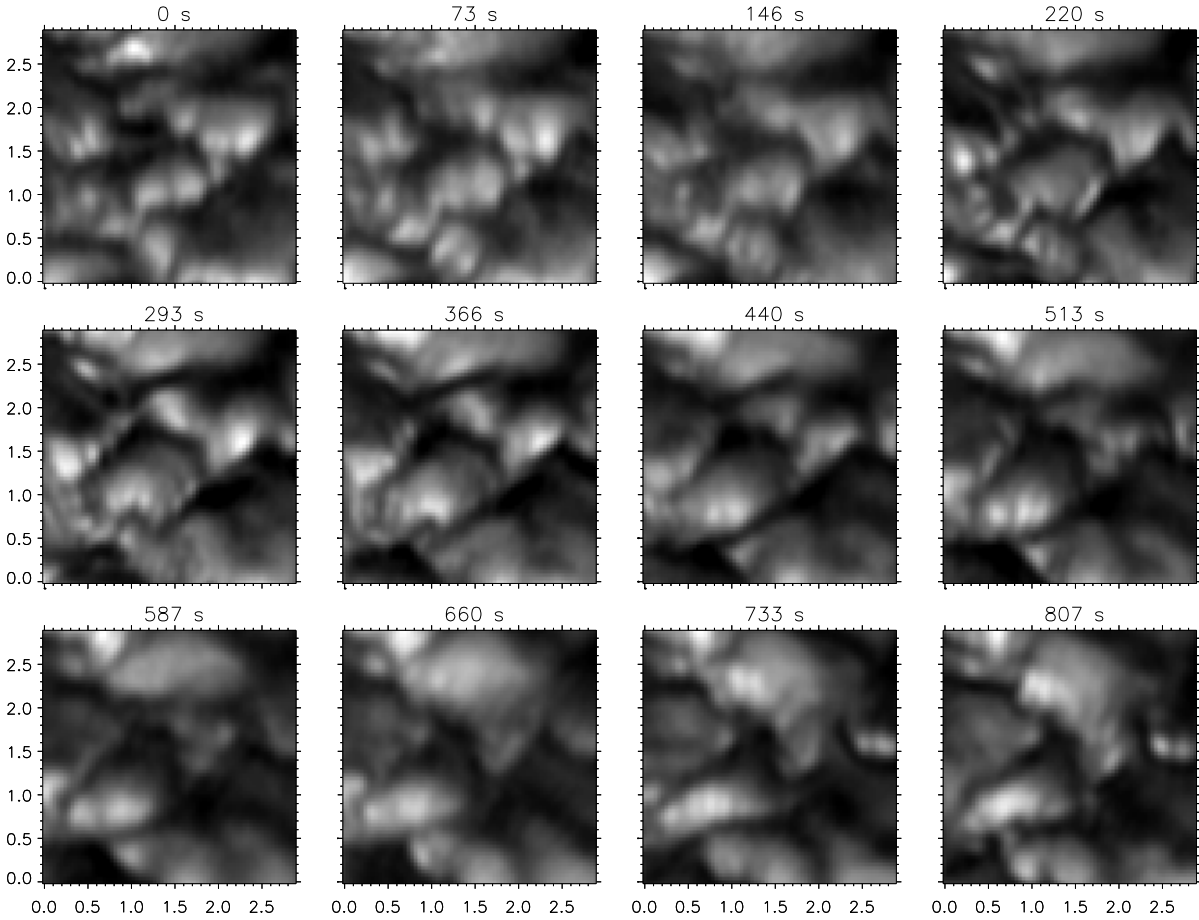


Fig. 3.— Typical example of dynamics of faculae in G-band images at very high spatial resolution. These 12 SST images show the evolution of a small patch ($2.8'' \times 2.8''$) of relatively dense plage (faculae) during 807 seconds. Bright facular elements (e.g., at $0.5''$, $1.5''$ at $t = 0$ s) do not retain their brightness or even identity over the course of several minutes. Most of the facular brightness changes are related to the evolution of granules in the vicinity of the facular elements. An mpeg movie is available online.

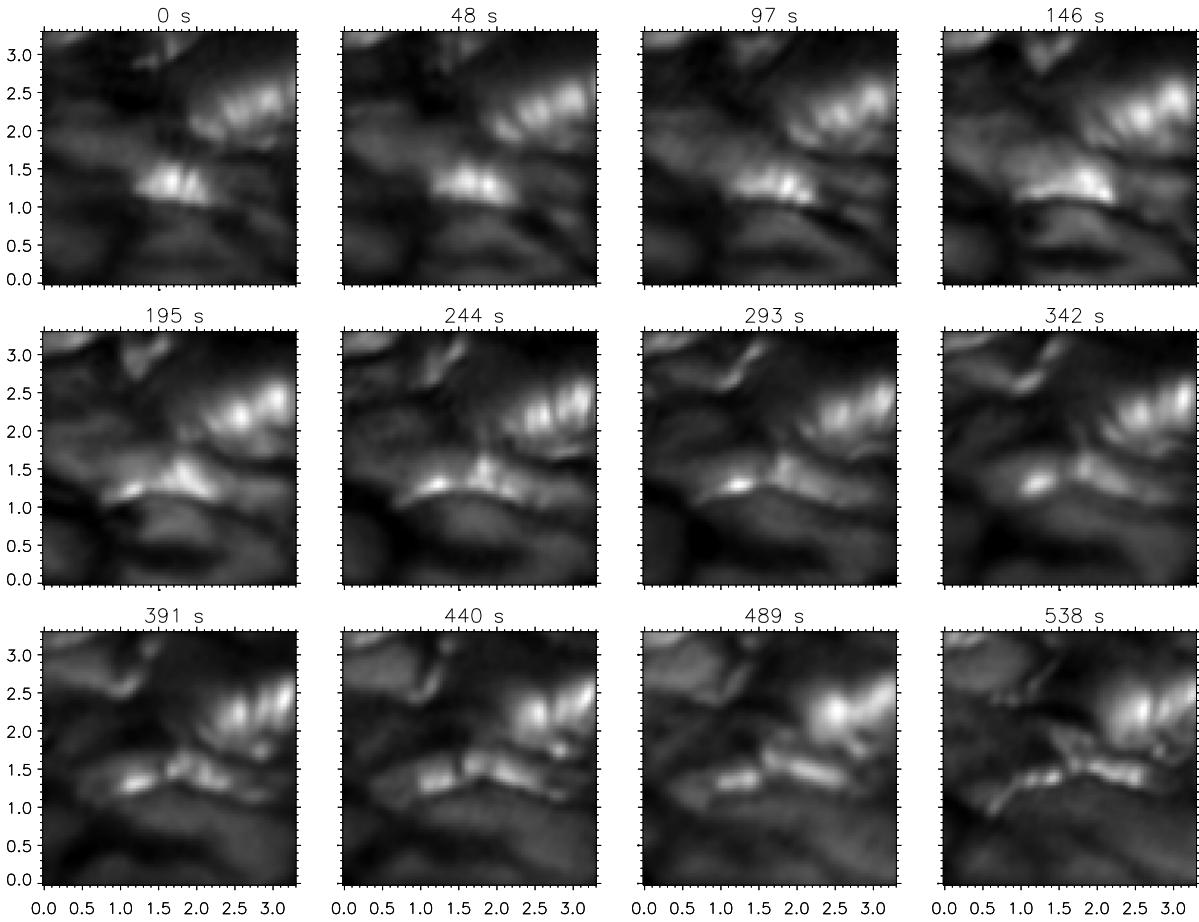


Fig. 4.— Spatially extended faculae change appearance to a thin line of pointlike brightenings in the course of less than 10 minutes in this SST data. Bright facular elements at $1.8''$, $1.2''$ (at $t = 0$ s) have been replaced by a thin line of bright points by $t = 538$ s. An mpeg movie is available online.

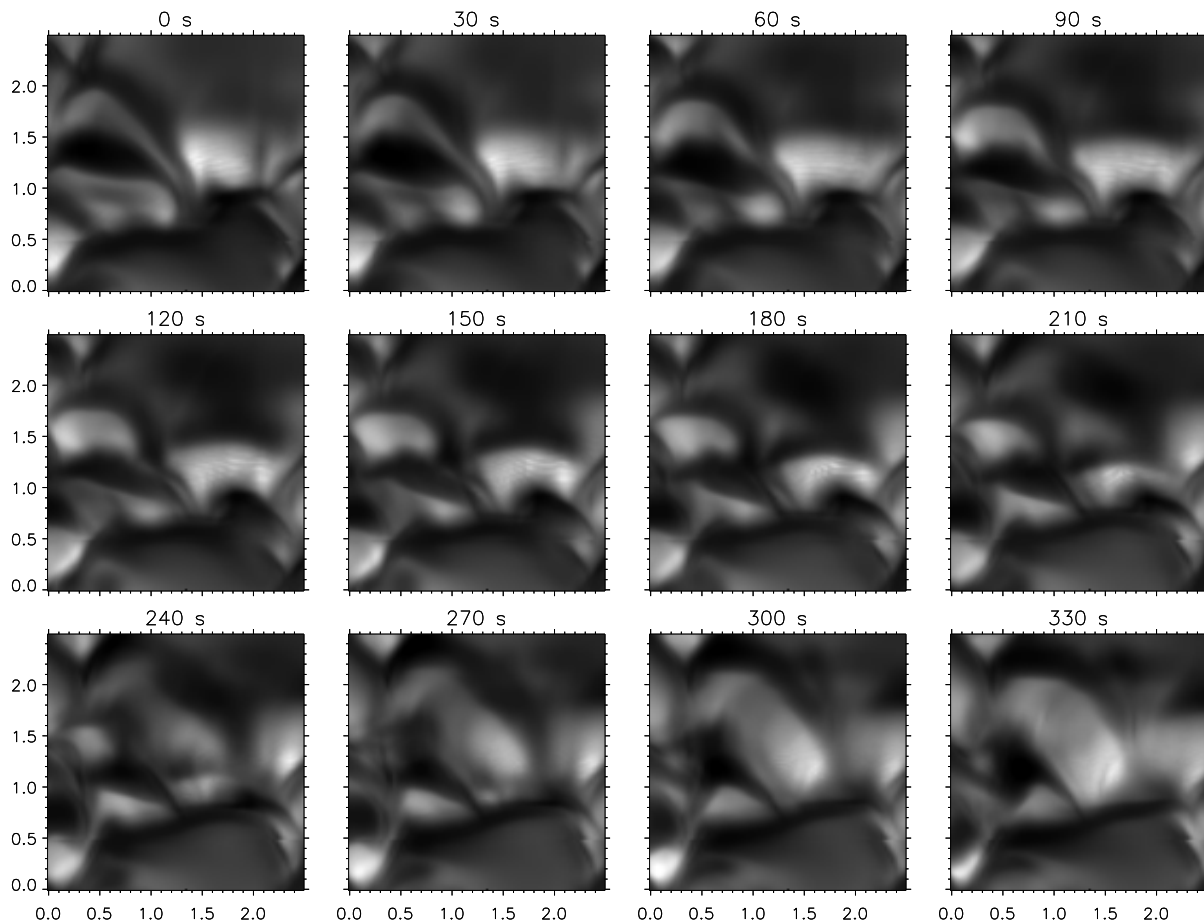


Fig. 5.— Facular dynamics as calculated by 3D radiative magneto-convective simulations. G-band 4302 Å images were synthesized with MULTI-3D and show the evolution of a small patch (2.4''x 2.4'') of plage (the limbward direction is up). The brightness and identity of almost all faculae varies drastically during the 5 minutes shown. These changes are caused by the changing temperature structure in the granules at the limbward side of the evacuated, lower opacity magnetic flux concentrations. An mpeg movie is available online.

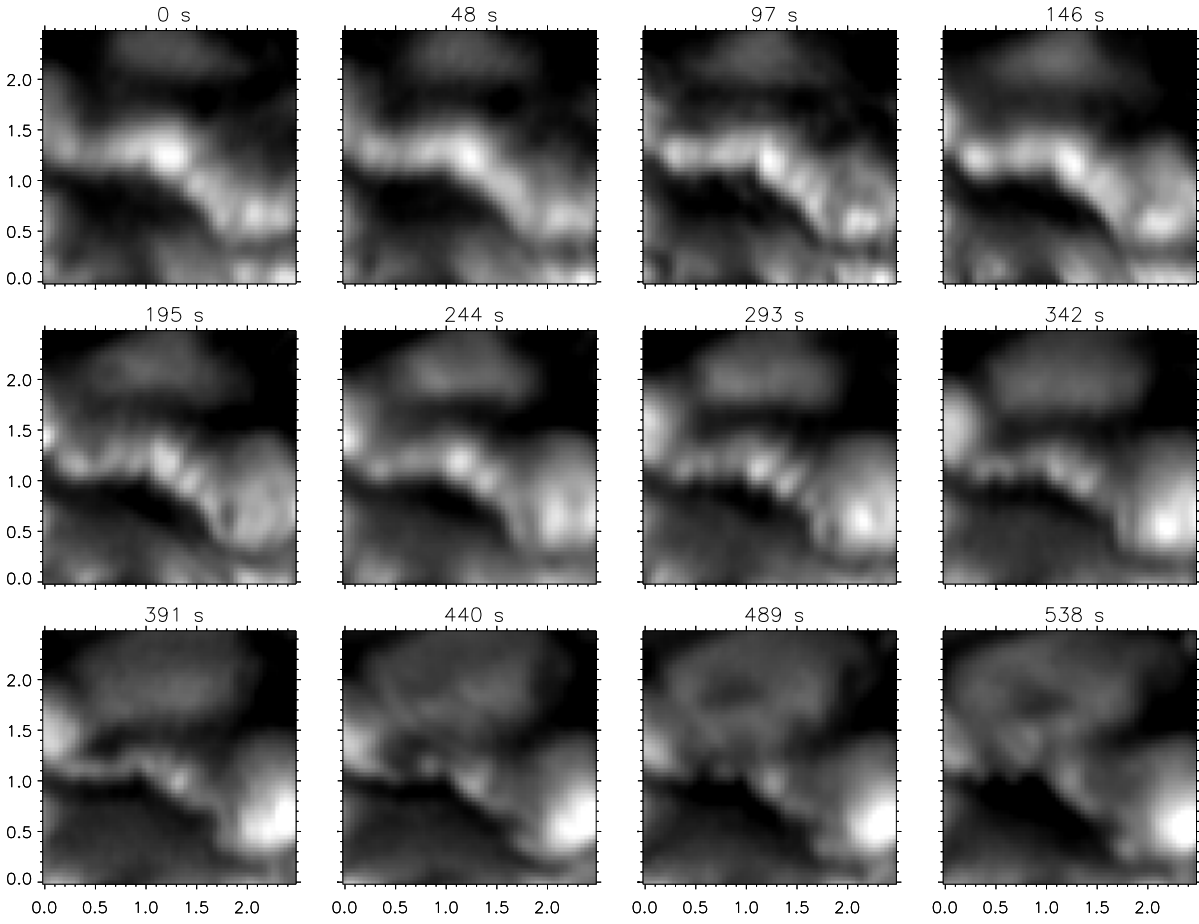


Fig. 6.— A dark band (at $0.5\text{-}2''$, $2''$) appears limbward of faculae in this SST data. The dark band gradually moves towards disk center (down), and seemingly sweeps over and "erases" the faculae temporarily, i.e., the facular brightness and limbward spatial extent gradually decrease until the faculae finally disappear. An mpeg movie is available online.

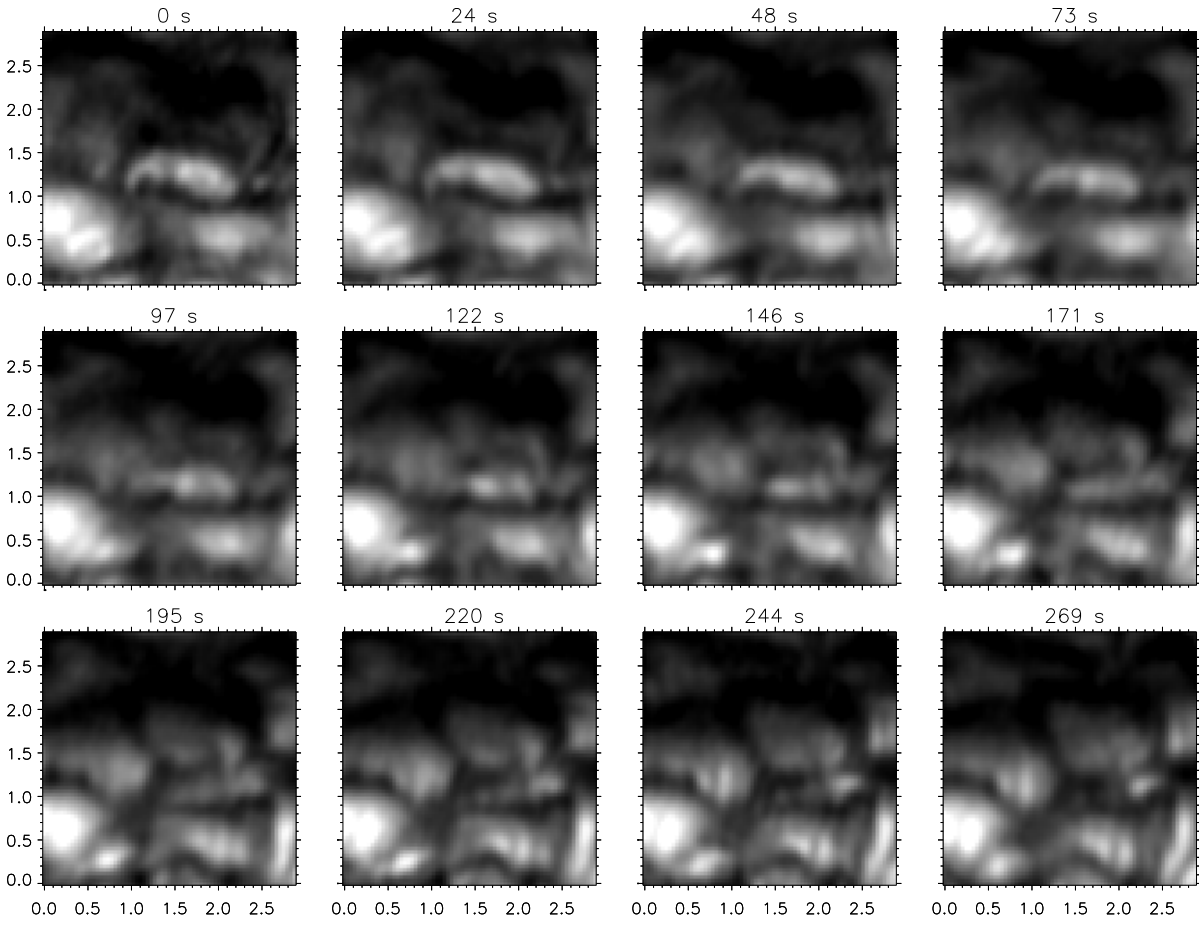


Fig. 7.— Another example of facular dynamics based on SST data in which a dark band (at 1-2.2", 1.5") appears to sweep over faculae, gradually decreasing the facular brightness and limbward spatial extent. Typically, facular brightness recovers within a few minutes after passage of the dark band (not shown here). An mpeg movie is available online.

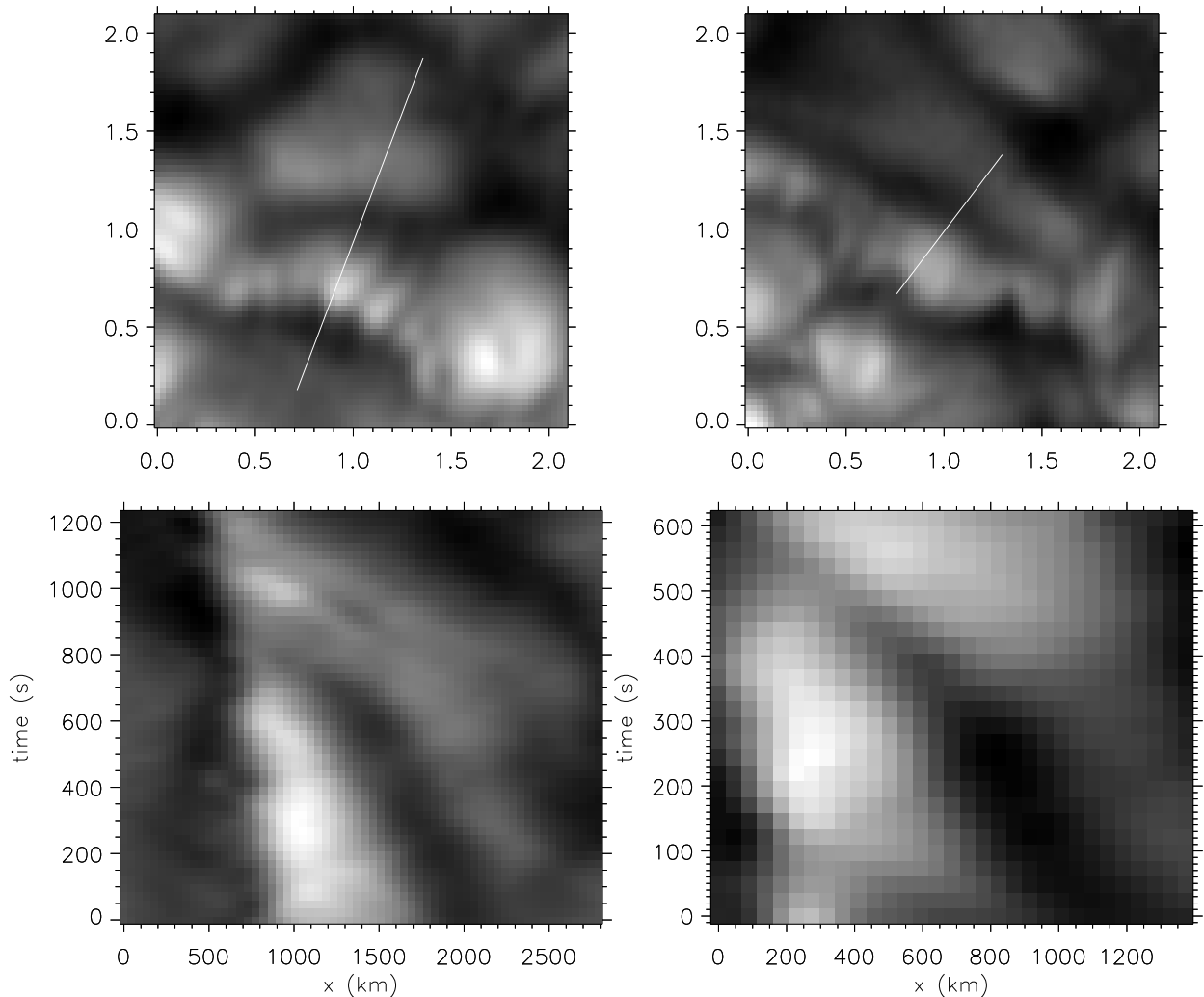


Fig. 8.— Top row: G-band SST images showing faculae swept over by a dark band. Full line shows where a cut is made to construct a space-time diagram (bottom row) for each case. The distance (in km) along the cut (white line, x-axis), is corrected for projection and reflects the distance on the solar surface. Time is shown on the y-axis. Both examples show how the faculae around 1200 km (left) and 300 km (right) become fainter as the dark lane approaches (for $t = 0$ s, at 2000 km and 1100 km respectively). By $t = 800$ s (left) and $t = 500$ s (right) the dark lane ”extinguishes” the faculae. The facular brightness seems to recover a few minutes later.

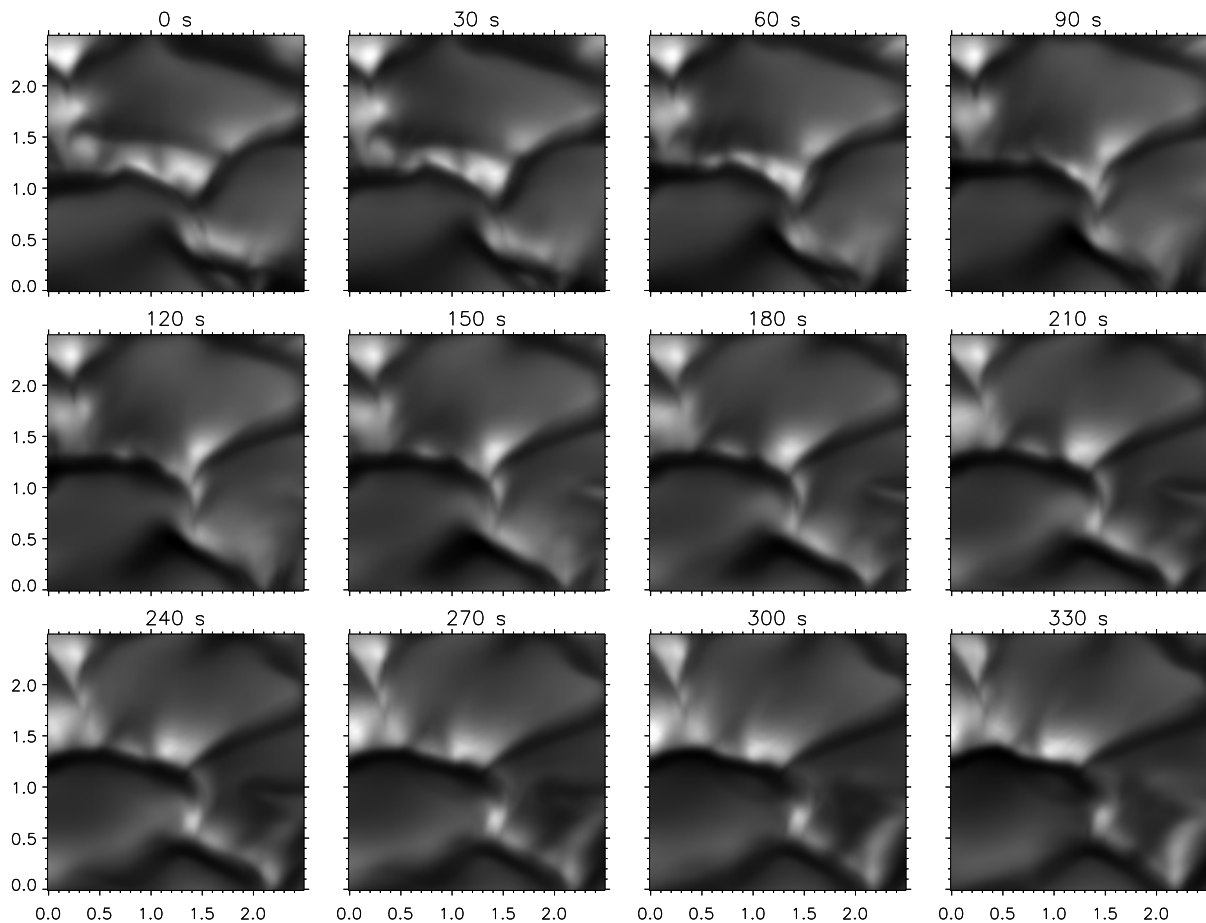


Fig. 9.— Facular dynamics as calculated by 3D radiative magneto-convective simulations. At $t = 0$ s a dark band is just above the center of the figure. It moves towards disk center (downwards in the figure) and the faculae are reduced to a weak band at $t = 90$ s. There is also a magnetic flux concentration advected by the granular flow starting at $(2.3'', 1.5'')$ at $t = 0$ s moving to the left and increasing in brightness while reaching position $(1.5'', 1.2'')$ at the end of the timeseries. An mpeg movie is available online.

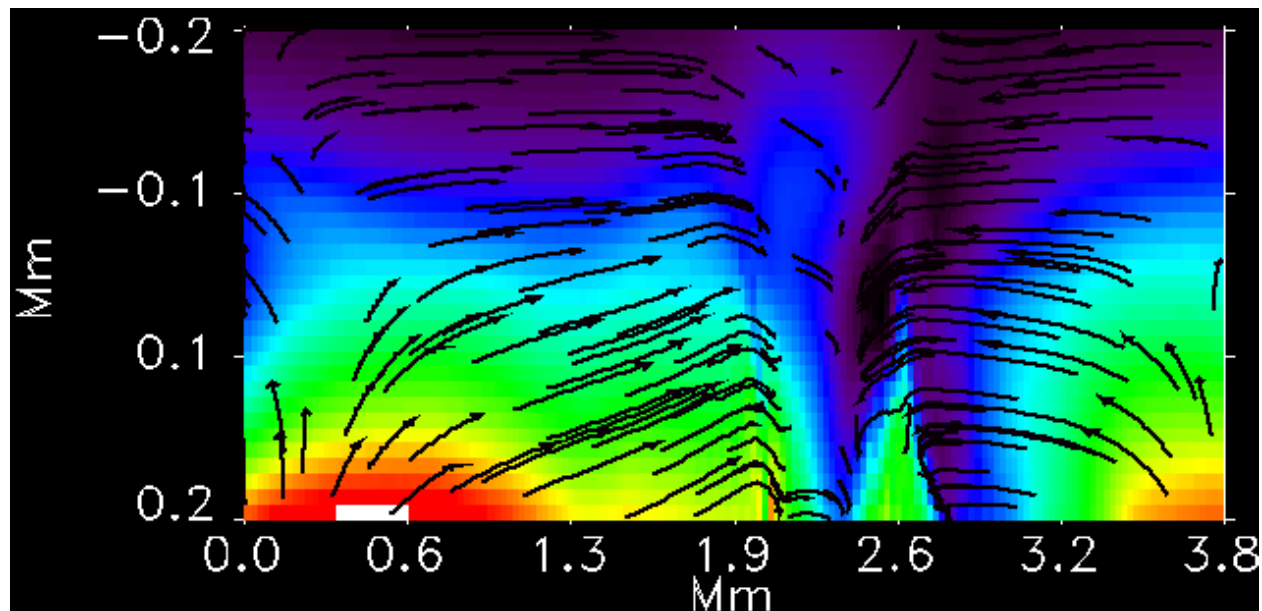


Fig. 10.— Image of total magnetic plus gas pressure fluctuations and superimposed fluid velocity vectors in a vertical slice perpendicular to a magnetic field filled intergranular lane. The high pressure near the granule center is pushing the granular upflows toward the intergranular lanes. Based on 3D magnetoconvective simulations. Tickmarks in Mm. An mpeg movie is available online.

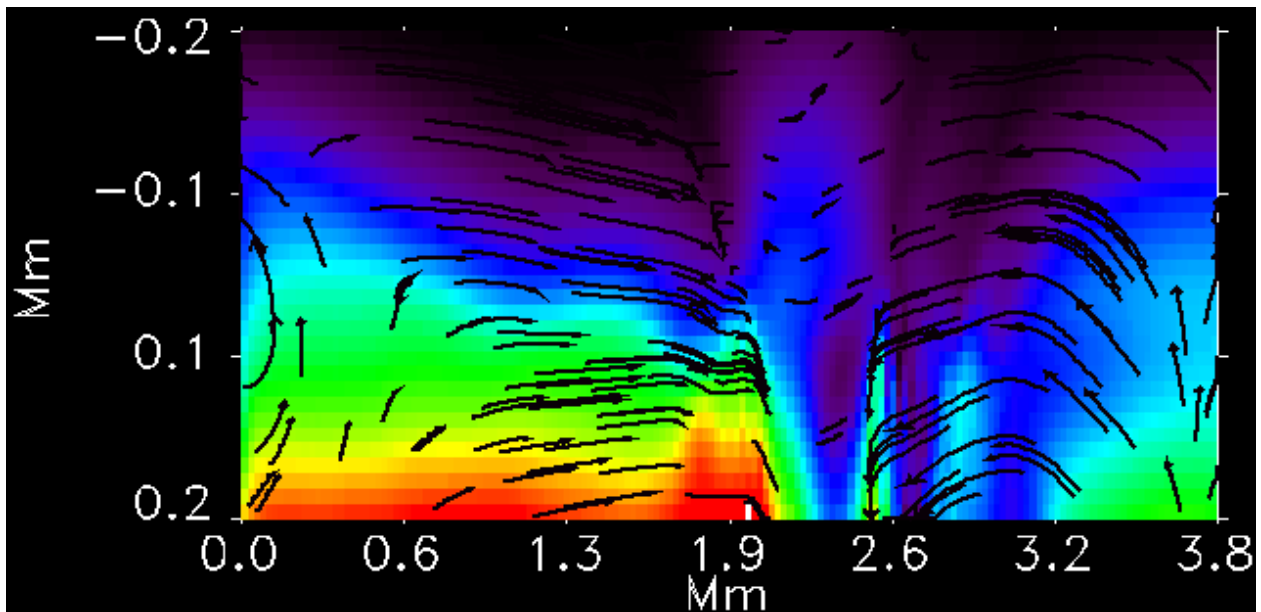


Fig. 11.— Image of total magnetic plus gas pressure fluctuations and superimposed fluid velocity vectors in a vertical slice perpendicular to a magnetic field filled intergranular lane 3 min after Fig. 10. The fluid flow has become nearly horizontal with wavelike undulation near the intergranular lane, which results in reduced or even downward convective energy flux. Based on 3D magnetoconvective simulations. The units of the x and y axis are in Mm.

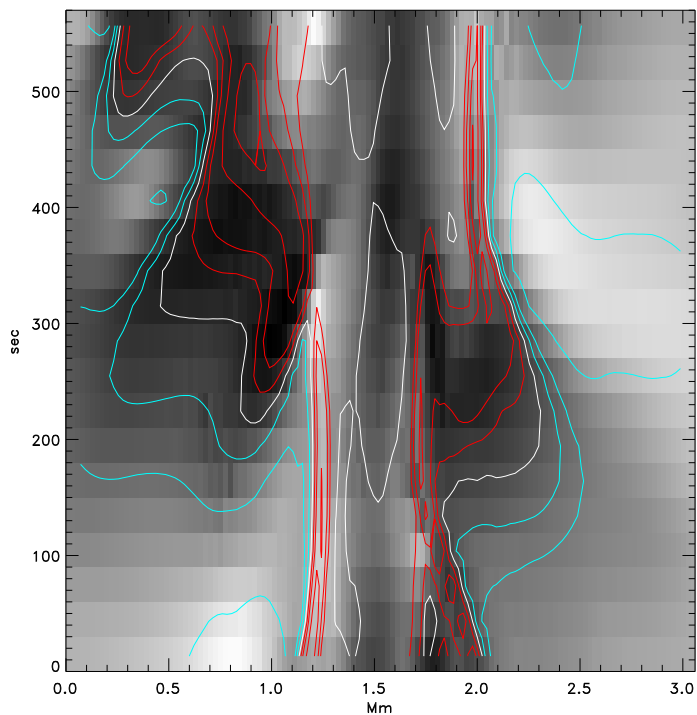


Fig. 12.— Space-time cut perpendicular to a dark band moving into faculae from 0.9 Mm at 220 s to 1.3 Mm at 370 s. The image is the continuum intensity along the cut, calculated from the 3D MHD simulation. The contours are the enthalpy plus kinetic energy flux at a depth of 100 km below $\langle \tau_{500} \rangle = 1$ (blue is upward, red is downward and white is zero). The dark band forms where the upward flux is reduced and becomes darker when the energy flux starts to remove energy from the surface layers.

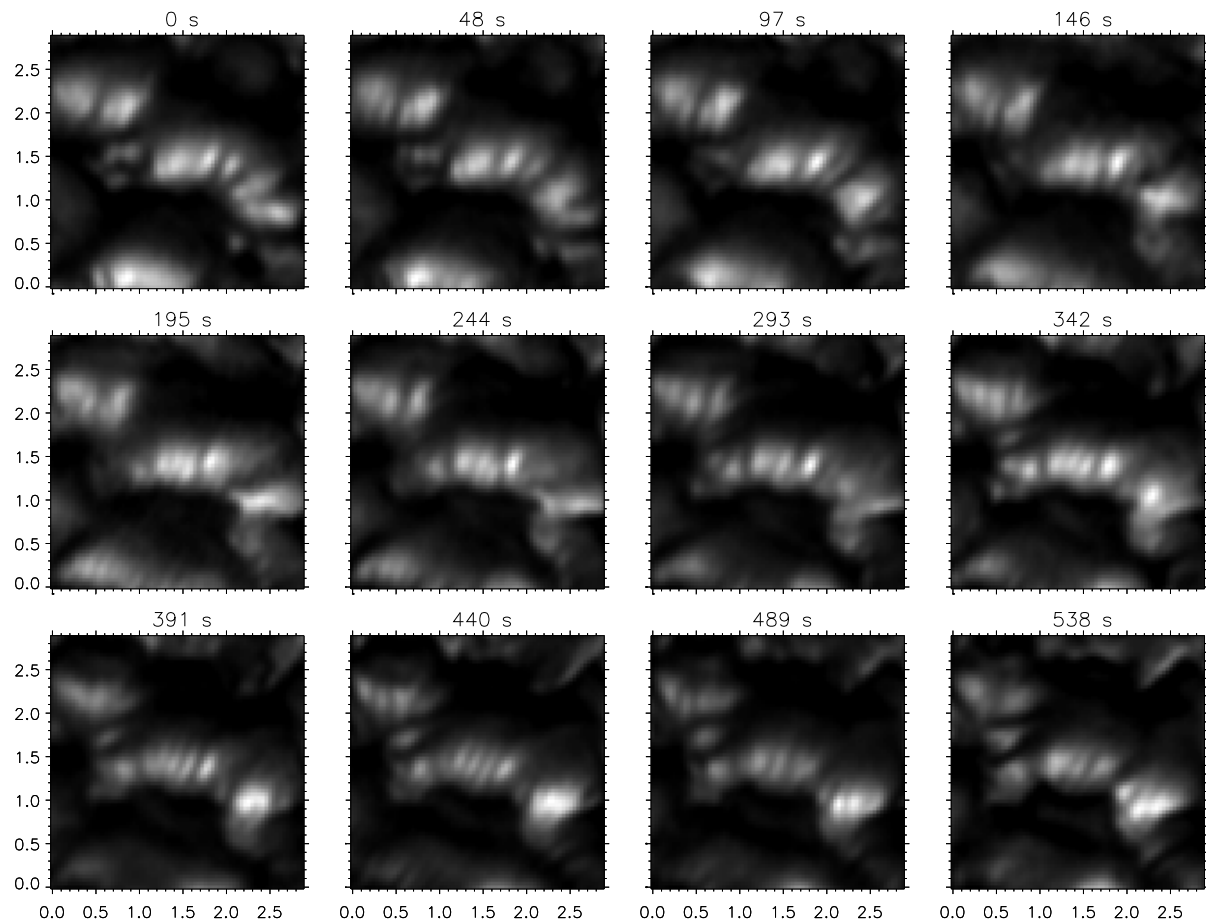


Fig. 13.— The location and number of striations of the striated facular elements around $(0.5'', 2'')$ and $(1.5'', 1.5'')$ is highly dynamic. This region was chosen for its relative lack of granular dynamics so that the overall presence of faculae is quite stable, allowing a detailed view of intrinsic facular variability. Based on SST data. An mpeg movie is available online.

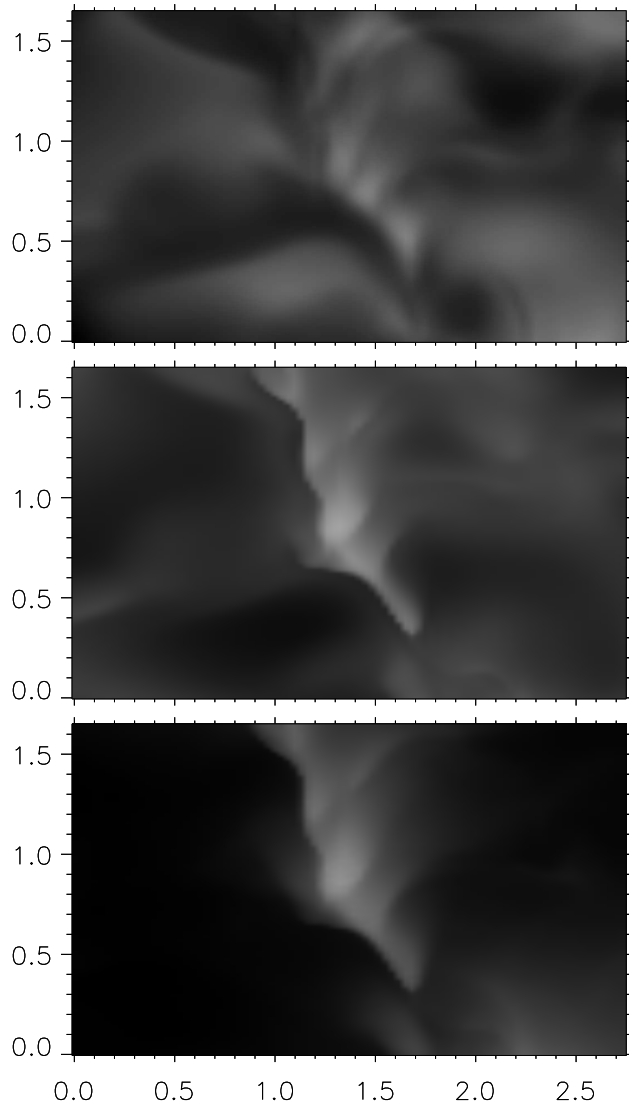


Fig. 14.— Top panel shows a synthetic G-band image viewed from $\mu=0.6$ based on a snapshot from 3D magnetoconvective simulations showing striated faculae. Middle panel shows the distance along the ray to optical depth unity with brighter corresponding to longer distance. The faculae correspond to positions where one can see further into the granule behind. The bottom panels shows the integrated magnetic field-strength along the ray down to optical depth unity. The dark gaps between bright facular striations correspond to lower integrated magnetic field strength. As explained in Carlsson et al. (2004), slanted rays through a region with strong magnetic field encounter lower density and opacity. Optical depth unity is then further into the granular wall where the temperature is higher. This explains why the distance (along the ray) to optical depth unity is correlated with stronger magnetic fields.

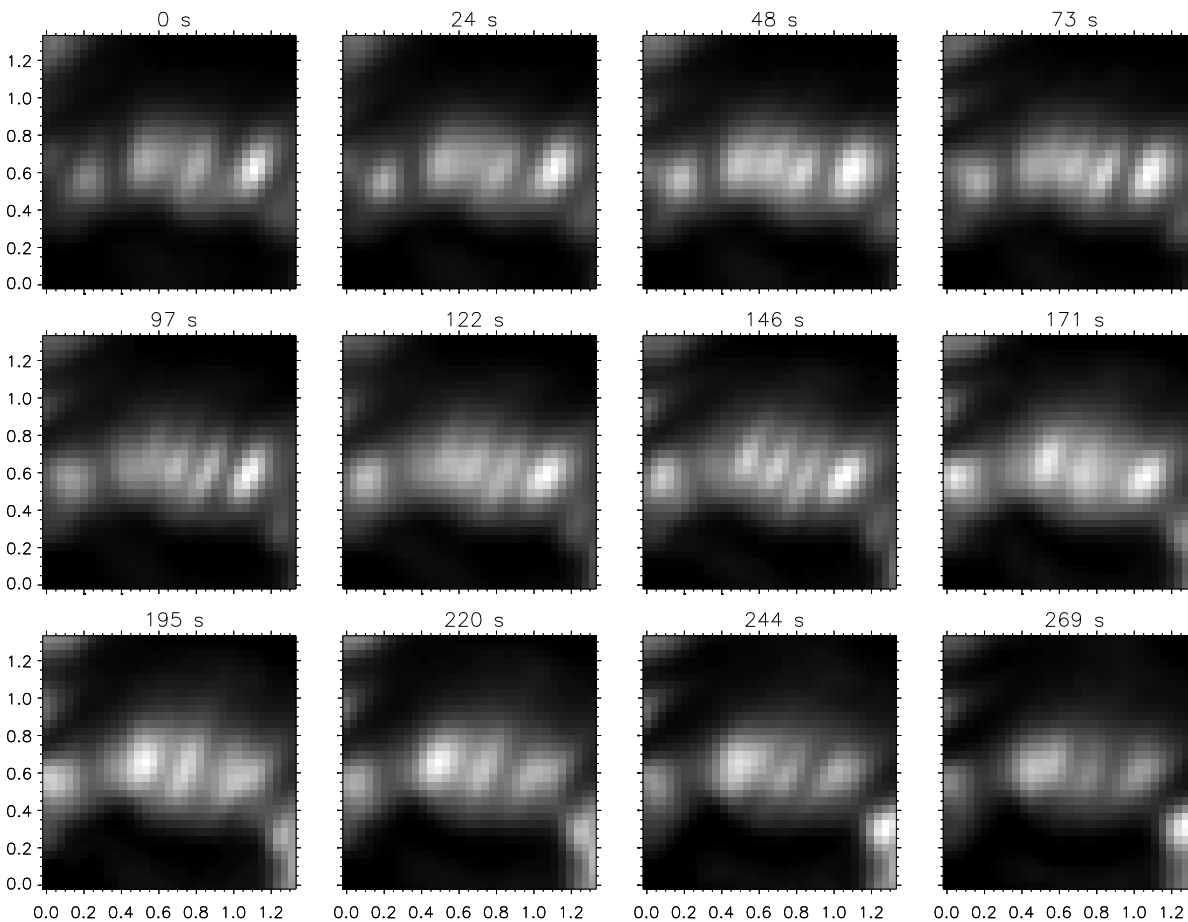


Fig. 15.— Another example of the dynamics of striated facular elements in a dense plage region where granular evolution is very slow. The striations merge, split and move rapidly in the direction perpendicular to their long axis. Based on SST data. An mpeg movie is available online.

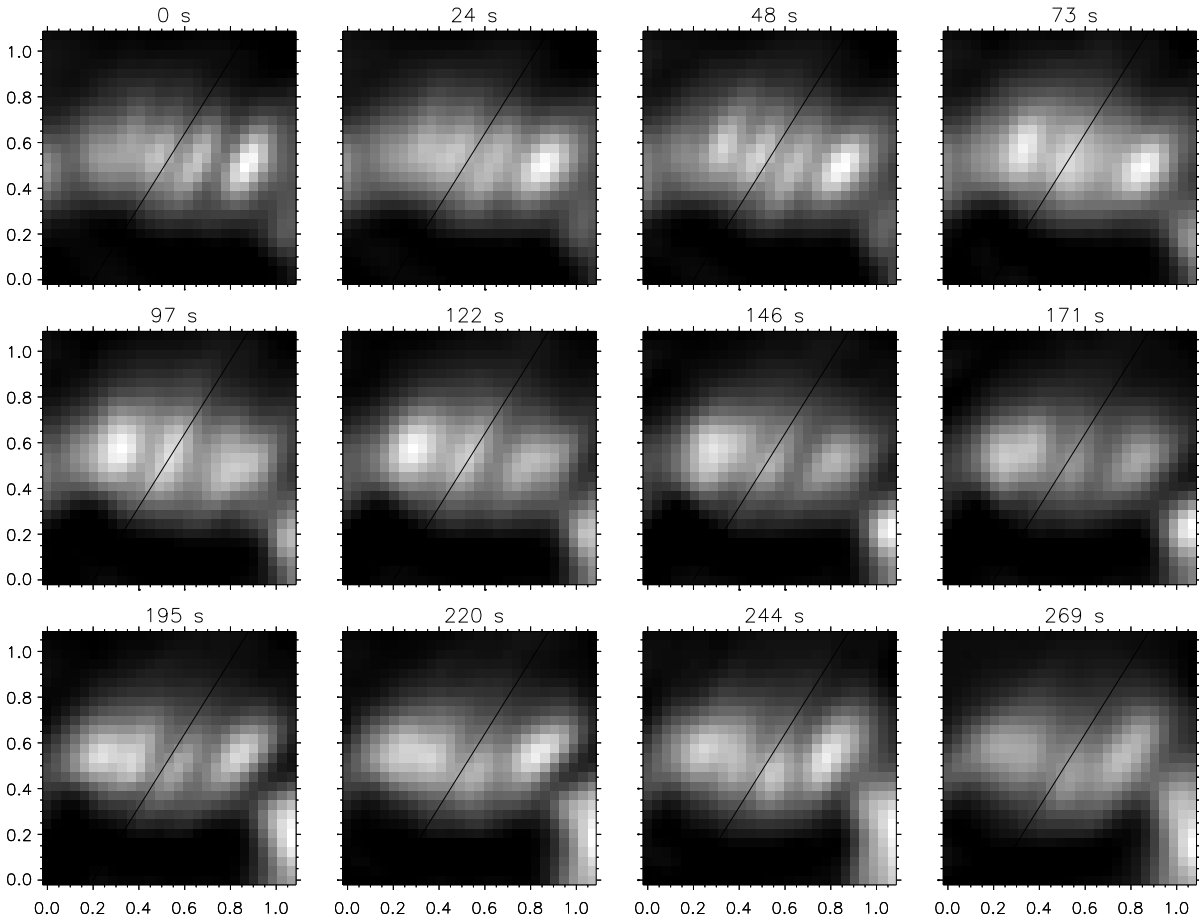


Fig. 16.— An example of "swaying" of a flux concentration in a dense plage region, where facular dynamics are more reflective of changes in the magnetic field than usual. Fluting and splitting dominates the faculae on timescales of order minutes. The black line is shown to guide the eye. Between 100 and 150 s, it appears some of the central facular striations undergo what looks like swaying. This is more clearly visible in the accompanying mpeg movie. Based on SST data.